Autoregulation of insulin receptor signaling through MFGE8 and the αvβ5 integrin

Ritwik Datta[a], Carlos O. Lizama[a], Amin K. Soltani[a,b], William Mckleroy[a,b,c], Michael J. Podolsky[a,c], Christopher D. Yang[a], Tony L. Huynh[d], Kelly M. Cautivo[e], Biao Wang[a,f], Suneil K. Koliwad[c,g], Nada A. Abumrad[h], and Kamran Atabai[a,b,c,f,1]

[a]Cardiovascular Research Institute, University of California, San Francisco, CA 94158; [b]Lung Biology Center, University of California, San Francisco, CA 94158; [c]Divisions of Pulmonary and Critical Care and Endocrinology, Department of Medicine, University of California, San Francisco, CA 94143; [d]Department of Radiology and Biomedical imaging, University of California, San Francisco, CA 94107; [e]Department of Laboratory Medicine, University of California, San Francisco, CA 94143; [f]Department of Physiology, University of California, San Francisco, CA 94158; [g]Diabetes Center, University of California, San Francisco, CA 94143; and [h]Diabetes Research Center, Department of Medicine and Cell Biology, Washington University in St. Louis, St. Louis, MO 63110

Edited by Mitchell A. Lazar, University of Pennsylvania, Philadelphia, PA, and approved March 11, 2021 (received for review February 5, 2021)

The role of integrins, in particular αv integrins, in regulating insulin resistance is incompletely understood. We have previously shown that the αvβ5 integrin ligand milk fat globule epidermal growth factor like 8 (MFGE8) regulates cellular uptake of fatty acids. In this work, we evaluated the impact of MFGE8 on glucose homeostasis. We show that acute blockade of the MFGE8/β5 pathway enhances while acute augmentation dampens insulin-stimulated glucose uptake. Moreover, we find that insulin itself induces cell-surface enrichment of MFGE8 in skeletal muscle, which then promotes interaction between the αvβ5 integrin and the insulin receptor leading to dampening of skeletal-muscle insulin receptor signaling. Blockade of the MFGE8/β5 pathway also enhances hepatic insulin sensitivity. Our work identifies an autoregulatory mechanism by which insulin-stimulated signaling through its cognate receptor is terminated through up-regulation of MFGE8 and its consequent interaction with the αvβ5 integrin, thereby establishing a pathway that can potentially be targeted to improve insulin sensitivity.

integrins | MFGE8 | insulin sensitivity | insulin receptor | insulin signaling

Acute insulin resistance can be viewed as a protective response under specific physiological conditions that necessitate increased insulin secretion. Nevertheless, the increasing prevalence of chronic insulin resistance (1) in the current obesity epidemic hastens the development of type 2 diabetes (T2D) and induces compensatory hyperinsulinemia. Hyperinsulinemia can produce potentially maladaptive consequences at least in part, due to the mitogenic roles of insulin (2–4). As such, there remains a critical need for new therapies to improve insulin sensitivity in order to prevent T2D, avoid the need for insulin treatment in patients with T2D, or reduce the insulin dose required to normalize blood glucose in such individuals.

Insulin binding to the alpha subunit of the insulin receptor induces a conformational change that triggers activation of insulin receptor beta subunit (IRβ) tyrosine kinase activity (5–7). The activated insulin receptor phosphorylates target molecules that mediate downstream signaling leading to glucose uptake and other metabolic effects (8, 9). Dephosphorylation of IRβ and insulin receptor substrate-1 (IRS-1) aids in termination of insulin signaling pathways (10, 11) and is the basis of clinical trials targeting putative phosphatases to treat diabetes (12). Despite their potential therapeutic relevance, there is a relative paucity of knowledge regarding molecular mechanisms that lead to termination of insulin receptor signaling.

The integrin families of cell surface receptors mediate bidirectional signaling between the cell and its external environment. Previous work has identified interactions between integrin receptors and other growth factor receptor tyrosine kinases (13–16) that lead to modulation of downstream signaling (17–19). For example, the αvβ3 and α6β4 integrins function as coreceptors for insulin-like growth factor-1 and 2 (IGF1 and 2) and potentiate IGF1 receptor (IGF1R)-mediated signaling (19–23). Immunoprecipitation studies have demonstrated a physical association between the αv integrins and IRβ (24, 25). The impact of these associations on glucose homeostasis has not been evaluated. A role for β1 integrins in the regulation of glucose homeostasis is well established. This class of integrins appears to be particularly important in regulating insulin-mediated glucose homeostasis in the obese state. The effect of β1 integrins on glucose homeostasis appears to be primarily due to obesity-associated matrix remodeling (26–30) rather than a direct effect secondary to a physical association between β1 integrins and the insulin receptor.

Milk fat globule epidermal growth factor like 8 (MFGE8) is a secreted integrin ligand which binds the αvβ3, αvβ5, and α8β1 integrins (31, 32). Several recent observations suggest a role for MFGE8 in modulating insulin resistance. In humans, serum MFGE8 levels are increased in the context of diabetes and correlate positively with the extent of hemoglobin glycosylation (33, 34). Indeed, serum MFGE8 levels correlate with indices of insulin resistance in two independent cohorts of patients with T2D or gestational diabetes from China (35, 36). A missense variation in the gene encoding MFGE8, present in South Asian Punjabi Sikhs, is associated with increased circulating MFGE8 levels and increased risk of developing T2D (37). Increased circulating levels of MFGE8 in diabetic patients may impact T2D through effects

Significance

The increasing prevalence of insulin resistance in the current obesity epidemic creates a significant need for ongoing investigations into the mechanisms that modulate insulin resistance. Long-term treatment of diabetic patients with high doses of insulin, especially in those that are obese, may cause further weight gain and exacerbate the risk of developing cancers. The work presented here demonstrates a previously unappreciated regulatory pathway by which insulin initiates dampening and/or termination of its own signaling pathway through an integrin-dependent pathway. These data identify a pathway that can potentially be targeted to reduce insulin requirements in patients with diabetes.

Author contributions: R.D., B.W., N.A.A., and K.A. designed research; R.D., C.O.L., A.K.S., W.M., C.D.Y., T.L.H., and K.M.C. performed research; S.K.K. contributed new reagents/analytic tools; R.D., C.O.L., M.J.P., and K.A. analyzed data; and R.D. and K.A. wrote the paper.

The authors declare no competing interest.

This article is a PNAS Direct Submission.

[1]To whom correspondence may be addressed. Email: kamran.atabai@ucsf.edu.

This article contains supporting information online at https://www.pnas.org/lookup/suppl/doi:10.1073/pnas.2102171118/-/DCSupplemental.

Published April 26, 2021.

on inflammation and cardiovascular disease. Humans with increased MFGE8 expression have a greater risk of developing coronary artery disease (38). In contrast, in murine models, MFGE8 deficiency exacerbates cardiac hypertrophy and atherosclerosis (39, 40). MFGE8 also improves wound healing responses in diabetic foot ulcers (41, 42) by triggering apoptotic cell clearance and promoting resolution of inflammation (43–45).

Despite the notable links between MFGE8, insulin resistance, and T2D pathology, the biology underlying these associations has not been investigated. We therefore evaluated the effect of acute antibody-mediated disruption of the MFGE8/β5 pathway on glucose homeostasis in wild-type (WT) mice. We report here that MFGE8 markedly attenuates the effect of insulin on skeletal muscle glucose uptake. Antibody-mediated blockade of MFGE8 or αvβ5 enhances while recombinant MFGE8 (rMFGE8) reduces insulin-stimulated glucose uptake in vitro and in vivo. Mechanistically, insulin acts to promotes cell-surface enrichment of skeletal muscle MFGE8, which then binds to cell surface αvβ5 and increases the interaction between the integrin and the insulin receptor. This interaction subsequently aids in terminating insulin receptor signaling.

Results

MFGE8 and the αvβ5 Integrin Dampen Insulin-Mediated Glucose Uptake. To determine whether the MFGE8/β5 pathway regulates glucose homeostasis, we performed a glucose tolerance test (GTT) in 8 wk old male WT mice in the presence of β5 blocking or isotype control antibody. β5 blockade significantly reduced serum glucose levels in WT mice as compared with isotype control antibody (Fig. 1*A*). Of note, antibody-mediated blockade of β5 did not affect glucose clearance in *Mfge8*$^{-/-}$ mice, indicating that MFGE8 functions upstream of β5 in regulating glucose uptake. Furthermore, *Mfge8*$^{-/-}$ mice used in the studies did not have altered glucose clearance in the GTT or body mass composition as compared with WT controls (Fig. 1*A* and *SI Appendix*, Fig. S1). Insulin levels during the GTT in the setting of β5 blockade correlated with blood glucose levels, suggesting that enhanced glucose clearance was not due to a direct effect of the blocking antibody on pancreatic insulin release (Fig. 1*B*). A GTT in WT mice conducted after intraperitoneal (IP) administration of an MFGE8 blocking antibody significantly enhanced (Fig. 1*C*) glucose clearance. By contrast, IP administration of rMFGE8 significantly blunted glucose clearance compared to treatment with control MFGE8 construct (RGE), carrying a single

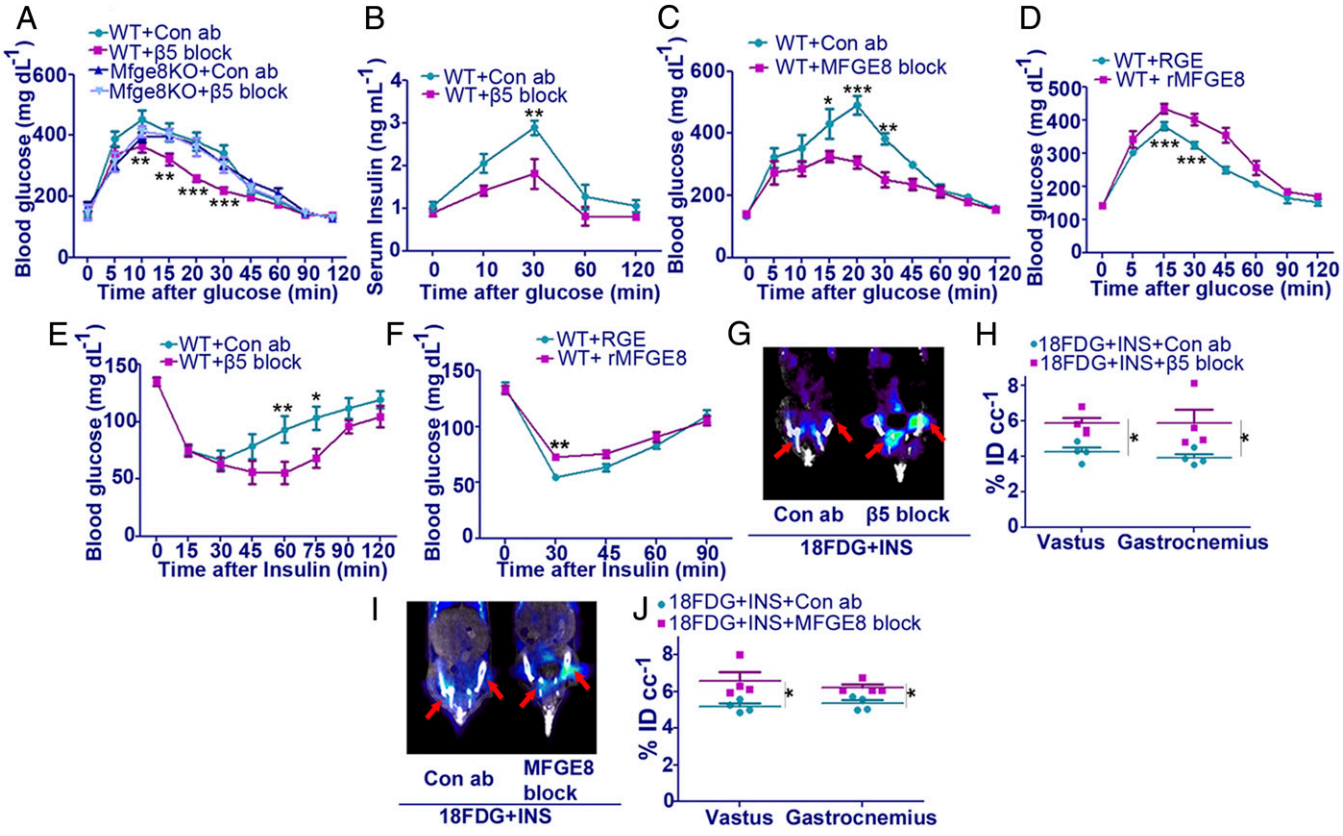

Fig. 1. MFGE8 regulates insulin-induced skeletal-muscle glucose uptake in vivo. (*A*) GTT in 7 to 8 wk old male WT and *Mfge8* $^{-/-}$ mice after IP injection of β5 blocking (β5 block) or isotype control antibody (Con ab). $n = 3$ to 4 for WT mice and $n = 3$ for *Mfge8* $^{-/-}$ mice per group per experiment and merged data from two to four independent experiments are presented. Statistical analysis compares the β5 blocking and control antibody groups in WT mice. (*B*) Serum insulin levels during GTT in WT mice. $n = 3$ to 4 mice per group per experiment, and merged data from two independent experiments are presented. (*C*) GTT in male WT mice after IP injection of MFGE8 blocking (MFGE8 block) or isotype control antibody (Con ab). $n = 3$ mice in each group per experiment, and merged data from two independent experiments are presented. (*D*) GTT in WT male mice after IP injection of recombinant MFGE8 (rMFGE8) or RGE control construct. $n = 2$ to 3 mice per group per experiment, and merged data from three independent experiments are presented. (*E*) ITT in WT male mice treated with β5 blocking or control antibody. $n = 3$ to 4 mice per group per experiment, and the merged data from four independent experiments are presented. (*F*) ITT after IP administration of rMFGE8 or RGE control in WT male mice. $n = 2$ to 3 mice per group per experiment, and merged data from three independent experiments are presented. (*G* and *I*) PET/CT scan images showing radioactive 18FDG deposition (red arrowheads) in 7 to 8 wk old WT male mice treated with β5 blocking, (*G*) MFGE8 blocking, (*I*) or control antibody in presence of insulin (1 U/kg) and 18FDG. $n = 4$ independent experiments. (*H* and *J*) Quantification of 18FDG deposition in vastus and gastrocnemius skeletal-muscle compartments in the setting of β5 (*H*) or MFGE8 (*J*) blockade. Data are expressed as % injected dose of 18FDG per cubic centimeter (cc) tissue (%ID cc^{-1}). All data expressed as mean ± SEM; $^{*}P < 0.05$, $^{**}P < 0.01$, and $^{***}P < 0.001$. Data in *A* through *F* were analyzed by two-way repeated measures ANOVA followed by Bonferroni's posttest. Data in *H* and *J* were analyzed by Mann–Whitney *U* test.

amino acid mutation that changes the RGD sequence to RGE (46) and precludes integrin binding (Fig. 1*D*).

The MFGE8/β5 Pathway Modulates Systemic and Skeletal Muscle Insulin Sensitivity. We next performed insulin tolerance tests and found that systemic β5 blockade significantly improved insulin tolerance (Fig. 1*E*) while treatment with rMFGE8 had the opposite effect (Fig. 1*F*) in WT male mice. Moreover, systemic β5 blockade significantly improved both glucose and insulin tolerance tests in female mice, indicating that the effects of targeting β5 generalizes across sex. (*SI Appendix*, Fig. S2 *A* and *B*). Taken together, these data suggest that the MFGE8/β5 pathway modulates insulin sensitivity in vivo.

To evaluate the effect of the MFGE8/β5 pathway on skeletal muscle insulin sensitivity, we treated WT mice with 18-fluoro-deoxy glucose (18FDG) and insulin after administering β5-blocking, MFGE8-blocking, or isotype control antibodies and then performed positron emission tomography/computed tomography (PET/CT) scanning. Systemic treatment with β5- or MFGE8-blocking antibodies significantly enhanced insulin-stimulated 18FDG uptake in hind-leg skeletal muscles (vastus lateralis, gastrocnemius). These data indicate that disruption of the MFGE8/β5 pathway enhances skeletal muscle glucose uptake in vivo (Fig. 1 *G*–*J*).

We tested whether these effects are cell intrinsic by examining the insulin-responsive uptake of a nonhydrolyzable fluorescent glucose analog, 2NBDG, in primary WT and *Mfge8*$^{-/-}$ skeletal muscle myotubes, human skeletal muscle myotubes (HskM), and differentiated C2C12 myotubes. In each system, rMFGE8 treatment dampened while β5 integrin blockade enhanced the ability of insulin to stimulate 2NBDG uptake. (Fig. 2 *A*–*C*). Moreover, *Mfge8*$^{-/-}$ myotubes had greater insulin-stimulated 2NBDG uptake than WT myotubes. This effect was reversed by treating the *Mfge8*$^{-/-}$ myotubes with rMFGE8, further supporting the concept that MFGE8 is a direct inhibitor of insulin-stimulated glucose uptake. By contrast, neither fibronectin nor vitronectin, two unrelated avβ5 integrin ligands, affected insulin-stimulated 2NBDG uptake in C2C12 myotubes (*SI Appendix*, Fig. S3), indicating that the effect of αvβ5 integrin on insulin-stimulated glucose uptake is specific to MFGE8. To further characterize these findings, we evaluated the effect of β5 blocking antibody on glucose uptake in response to a dose range of insulin in C2C12 myotubes. We found a similar and significant effect of β5 blockade on glucose uptake at insulin doses of 100 and 200 nM (Fig. 2*D*). We also performed a time course experiment in this system and found a significant effect of β5 blockade on glucose uptake beginning 30 min after insulin administration that persisted at 45 and 60 min after insulin administration (Fig. 2*E*).

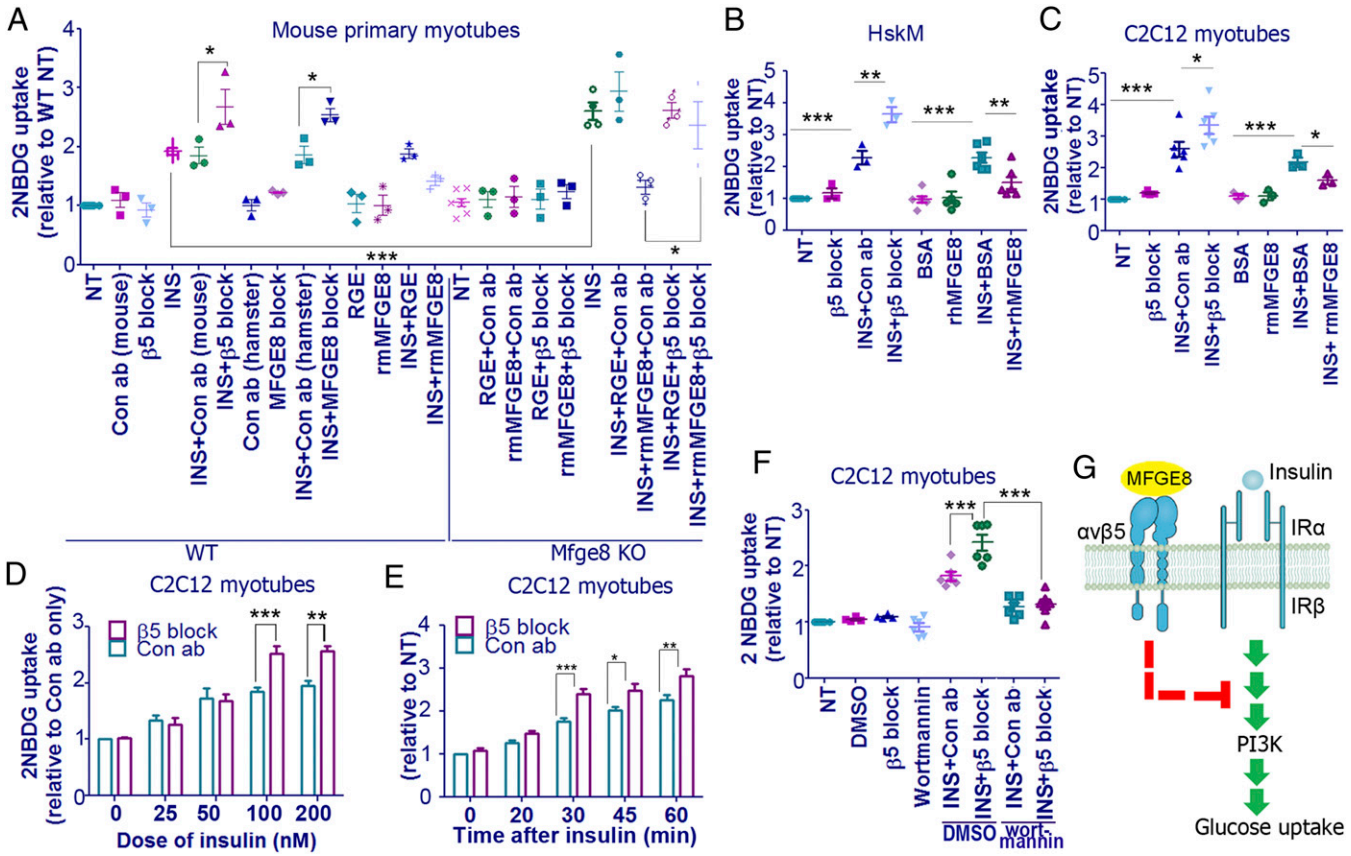

Fig. 2. MFGE8 regulates insulin-induced glucose uptake in vitro. (*A*–*C*) 2NBDG uptake assay in mouse primary *WT* and *Mfge8*$^{-/-}$ myotubes (*A*, $n = 3$ independent experiments), primary HsKM (*B*, $n = 3$ to 6 independent experiments), and differentiated C2C12 myotubes (*C*, $n = 3$ to 6 independent experiments) in the presence or absence of rMFGE8 or RGE control protein, β5 blocking, MFGE8 blocking, or isotype control antibody and insulin (100 nM). Data are expressed as relative fold changes compared to the untreated cells (NT). (*D* and *E*) Dose response (*D*, $n = 4$ to 6 independent experiments) and time course of insulin action (*E*, $n = 6$ independent experiments) on 2NBDG uptake in C2C12 myotubes in the presence of either β5 blocking or control antibody. Data are expressed as relative fold changes compared to control antibody-treated cells in the absence of insulin. (*F*) 2NBDG uptake assay in β5 blocking antibody–treated C2C12 cells in the presence and absence of insulin and wortmannin. Data are expressed as relative fold changes compared to the untreated cells (NT). $n = 4$ to 6 independent experiments. $^*P < 0.05$, $^{**}P < 0.01$, and $^{***}P < 0.001$. Data analyzed by one-way ANOVA followed by Bonferroni's posttest (*A*, *D*, and *F*). Data in *E* were analyzed by two-way repeated measures ANOVA followed by Bonferroni's posttest. (*G*) Proposed model of how the MFGE8/β5 pathway dampens insulin-stimulated glucose uptake.

Insulin stimulates glucose uptake in the myotubes via canonical activation of PI3 kinase pathway (47–50). To determine whether the enhanced insulin sensitivity by β5 blockade is sensitive to PI3K inhibition, we examined insulin-stimulated 2NBDG uptake in C2C12 myotubes treated with β5 blocking antibody in the presence of PI3K inhibitor wortmannin. Wortmannin significantly dampened insulin-stimulated 2NBDG uptake (Fig. 2*F*). β5 blockade failed to augment insulin-stimulated glucose uptake in the presence of wortmannin, indicating that β5 blockade potentiates the PI3K/AKT pathway to trigger glucose uptake in these cells (Fig. 2*F*). Taken together, these data indicate that MFGE8 and β5 integrin limit insulin-stimulated glucose uptake via regulation of canonical insulin signaling pathway in a cell-intrinsic manner (Fig. 2*G*).

To investigate whether augmented insulin signaling due to β5 blockade promotes tumor growth, we assessed cell proliferation of MCF-7 human breast-cancer cells treated with β5 blocking antibody in the presence or absence of insulin. Incubation of MCF-7 cells with β5 blocking antibody (with or without insulin administration) for 6 h induced marked cell death, as measured by propidium iodide staining followed by flow cytometry, mitigating concerns of β5 blockade promoting tumor growth (*SI Appendix*, Fig. S4).

MFGE8 and the αvβ5 Integrin Regulate Insulin Receptor Signaling in Skeletal Muscle. We next investigated whether the MFGE8/β5 integrin pathway regulates insulin receptor signaling. We measured the impact of antibody-mediated β5 blockade on insulin-stimulated tyrosine phosphorylation of IRβ and IRS-1 in C2C12 myotubes. We pretreated C2C12 myotubes with β5 blocking or control antibody for 1 h, followed by insulin for 5 or 30 min. Subsequent immunoprecipitation of protein lysates using an anti–phospho-tyrosine antibody, followed by Western blotting for IRβ and IRS-1, demonstrated that β5 blockade enhanced insulin-stimulated tyrosine phosphorylation of IRβ and IRS-1 at both time points (Fig. 3*A*). We repeated experiments at the 30 min time point with a dose range of insulin (25, 50, 100, and 200 nM) and observed enhanced tyrosine phosphorylation of IRβ and IRS-1 at each of these doses after β5 blockade (Fig. 3*B* and *SI Appendix*, Fig. S5 *A–C*). Additionally, treatment of C2C12 myotubes with rMFGE8 but not RGE control construct blunted insulin-stimulated tyrosine phosphorylation of IRβ and IRS-1, indicating that the effect of rMFGE8 treatment is dependent on integrin binding (Fig. 3*C*).

To extend these findings in vivo, we administered β5 blocking or control antibody to WT mice 1 h before treatment with IP insulin, harvested hind-leg skeletal muscles 15 and 60 min after insulin treatment, and performed immunoprecipitation of protein lysates using an anti–phospho-tyrosine antibody followed by Western blotting for IRβ and IRS-1. β5 blockade led to persistent tyrosine phosphorylation of both IRβ and IRS-1 in skeletal muscle (Fig. 3*D*). Taken together, these data indicate that targeted disruption of the MFGE8/β5 pathway potentiates insulin receptor activation and signaling in vitro and in vivo.

αvβ5 Integrin Regulates Hepatic Insulin Signaling. To determine whether our findings extended beyond the skeletal muscle system, we assessed the effect of β5 blockade in the hepatic system. We performed a pyruvate tolerance test (PTT) in 6 wk old male WT mice in the presence of β5 blocking or isotype control antibody. β5 blockade significantly suppressed the rise in blood glucose levels in WT mice after administration of pyruvate (Fig. 4*A*). We next treated HepG2 liver cells and primary hepatocytes with insulin for 30 min in the presence of β5 blocking or control antibody and performed coimmunoprecipitation using a phospho-tyrosine antibody followed by Western blotting for IRβ and IRS-1. We found that β5 blockade potentiated insulin receptor signaling in response to insulin in both HepG2 (Fig. 4 *B–D*) and primary hepatocytes (Fig. 4*E*). We performed similar coimmunoprecipitation experiment from total liver lysates of mice treated with insulin for 15 and 60 min in the presence of β5 blocking or control antibody. In this system, β5 blockade significantly enhanced phosphorylation of IRβ and IRS-1 at the 15 min time point but not at the 60 min time point (Fig. 4 *F–H*). We also evaluated whether prolonged treatment with β5 blocking antibody (weekly administration for a total of 8 wk) impacted liver fat content and found no differences in liver triglyceride content or serum triglycerides (*SI Appendix*, Fig. S6 *A* and *B*). Taken together, these data indicate that

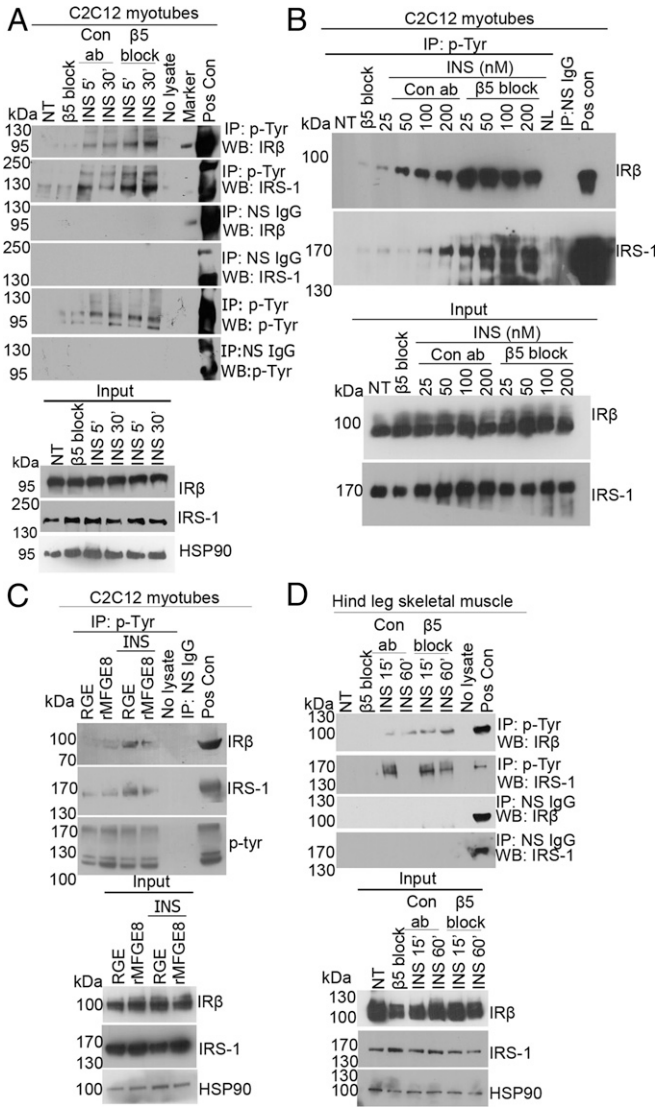

Fig. 3. Persistent activation of insulin receptor signaling with disruption of the MFGE8/β5 pathway in skeletal muscle. (*A–C*) Coimmunoprecipitation experiments demonstrating the effect of β5 blockade and rMFGE8 treatment on IRβ and IRS-1 tyrosine phosphorylation in presence or absence of insulin (INS). (*A*) C2C12 myotubes were treated with insulin (100 nM) for 5 min (INS 5′) or 30 min (INS 30′) in presence of either β5 (*A*) blocking or isotype control antibody or (*C*) rMFGE8 or RGE protein coadministered with insulin. Western blots are representative of three independent experiments. (*B*) Dose response of insulin action on IRβ and IRS-1 tyrosine phosphorylation in presence of β5 blocking or isotype control antibody. Western blots are representative of four independent experiments. (*D*) Coimmunoprecipitation studies showing tyrosine phosphorylation of IRβ and IRS-1 in skeletal-muscle lysates from WT mice treated with IP insulin (1 U/kg) for 15 min (INS 15′) or 60 min (INS 60′) in presence of β5 blocking or control antibody. Western blots are representative of three independent experiments. WT male mice were used for all in vivo experiments.

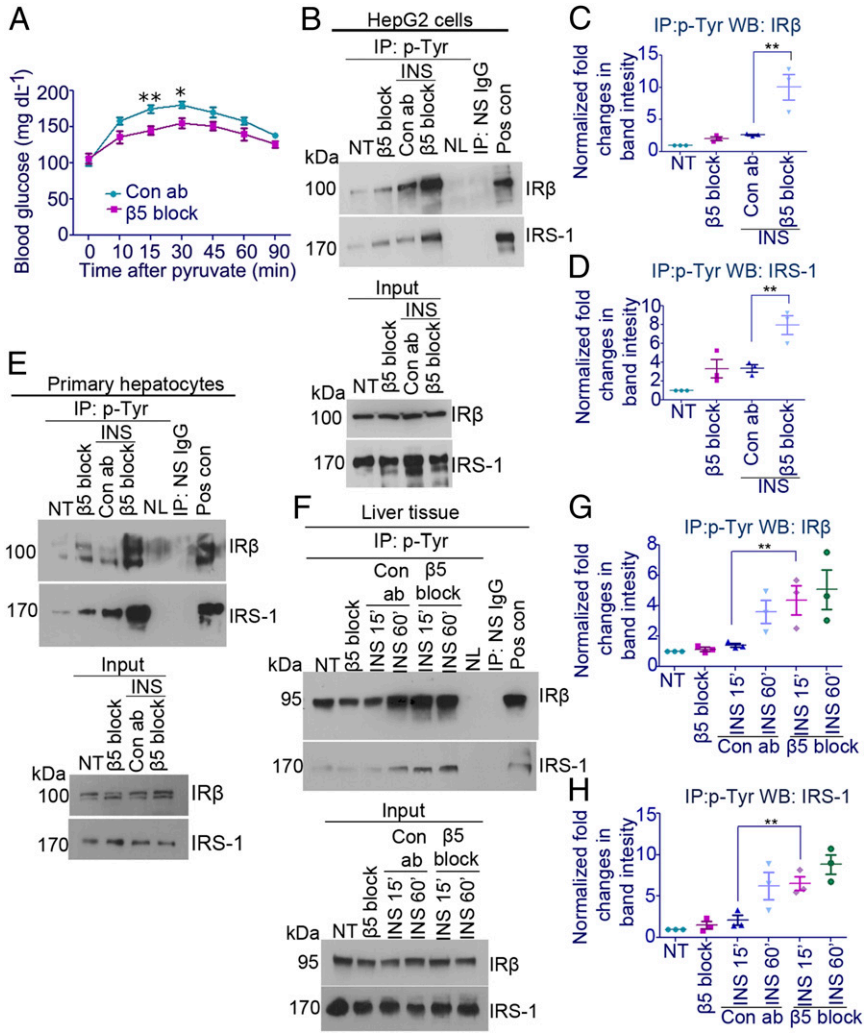

Fig. 4. Enhanced hepatic insulin sensitivity after β5 blockade. (*A*) PTT in 6 wk old male WT mice after IP injection of β5 blocking (β5 block) or isotype control antibody (Con ab). $n = 3$ to 4 in each group per experiment; data merged from two independent experiments are presented. (*B*) Coimmunoprecipitation experiments demonstrating the effect of β5 blockade on IRβ and IRS-1 tyrosine phosphorylation in the presence or absence of insulin (INS,100 nM for 30 min) in HepG2 cells after treatment with β5 blocking or isotype control antibody. Western blots are representative of three independent experiments. (*C* and *D*) Densitometric analysis of the Western blots (including *B*) of IRβ and IRS-1 tyrosine phosphorylation in HepG2 cells. (*E*) Coimmunoprecipitation experiments demonstrating the effect of β5 blockade on IRβ and IRS-1 tyrosine phosphorylation in the presence or absence of insulin (INS,100 nM for 30 min) in murine primary hepatocytes in the presence of β5 blocking or isotype control antibody. Western blots are representative of three independent experiments. Both male and female mice were used for primary hepatocyte isolation. (*F*) Coimmunoprecipitation studies showing IRβ and IRS-1 tyrosine phosphorylation from liver lysates of WT male mice treated with IP insulin (1 U/kg) for 15 min (INS 15′) or 60 min (INS 60′) in the presence of β5 blocking or control antibody. Western blots are representative of three independent experiments. (*G* and *H*) Densitometric analysis of Western blots (including *F*) showing fold changes in IRβ and IRS-1 tyrosine phosphorylation relative to NT. $^{*}P < 0.05$ and $^{**}P < 0.01$. Data in *A* were analyzed by two-way repeated measures ANOVA followed by Bonferroni's posttest. Data in *C*, *D*, *G*, and *H* were analyzed by one-way ANOVA followed by Bonferroni's posttest.

the effects of the MFGE8/β5 integrin pathway on insulin signaling extend beyond the skeletal system to the liver.

Association between the αvβ5 Integrin and IRβ. We next evaluated whether the αvβ5 integrin is part of a complex with the insulin receptor. First, we immunostained for β5 and IRβ in untreated and insulin-treated C2C12 myotubes. IRβ and β5 colocalized, and colocalization increased with insulin treatment (*SI Appendix*, Fig. S7). Next, we performed a proximity ligation assay (PLA) in differentiated C2C12 and HsKM myotubes observing a positive signal for proximity between β5 and IRβ that was markedly increased 30 min after insulin treatment (Fig. 5*A*). β5 blockade reduced the PLA signal at baseline and after insulin treatment (Fig. 5*A*). We also performed coimmunoprecipitation studies of C2C12 cellular lysates using an antibody targeting the cytoplasmic domain of β5 and probing the pulldown product for IRβ. Consistent with our PLA results, we observed a baseline association between β5 and IRβ, which was enhanced with insulin stimulation. Furthermore, the baseline and insulin-stimulated association was reduced with β5 blockade (Fig. 5 *B* and *C*) and enhanced by rMFGE8 (Fig. 5 *D* and *E*). These findings indicate that αvβ5 integrin associates with IRβ and that both insulin and MFGE8 strengthen this association.

To validate these findings in vivo, we administered β5 blocking or isotype control antibody in WT mice 1 h before IP insulin treatment and then performed the same immunoprecipitation studies from hind-leg skeletal muscle lysates after insulin treatment. We observed a baseline association between β5 and IRβ that increased markedly 60 min after IP insulin treatment (Fig. 5 *F* and *G*). Pretreatment with the β5 blocking antibody significantly reduced this association 60 min after insulin stimulation (Fig. 5 *F* and *G*). We also immunostained for IRβ and β5 in hind-leg skeletal muscles of mice treated with insulin for 60 min in the presence of β5 blocking

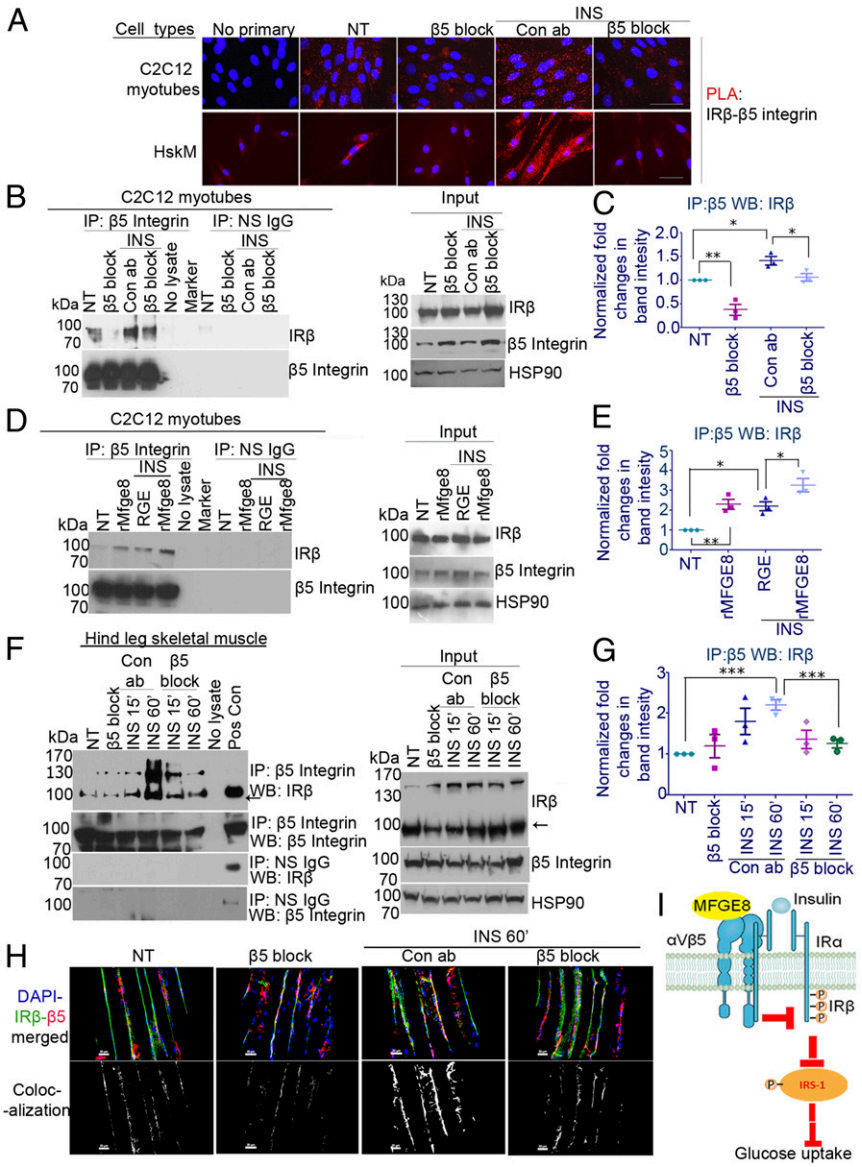

Fig. 5. Interaction between IRβ and the β5 integrin. (*A*) PLA showing proximity between IRβ and β5 in C2C12 myotubes and primary HskM treated with β5 blocking or isotype control antibody and with or without 30 min of insulin (INS, 100 nM) treatment. $n = 3$ for C2C12, and $n = 2$ for HsKM myotubes. (Scale bar, 5 μm.) Magnification of 60× for C2C12 myotubes; 40× magnification for HsKM. (*B–E*) Coimmunoprecipitation experiments and respective densitometric analyses demonstrating the effect of β5 blockade (*B* and *C*) and rMFGE8 treatment (*D* and *E*) on the interaction between IRβ and β5 in the presence or absence of insulin (INS, 100 nM) using an antibody recognizing the cytosolic domain of β5 antibody for pulldown and subsequent Western blot for IRβ. Western blots are representative of three independent experiments. Densitometric data represented as fold changes relative to no treatment group (NT). (*F*) Coimmunoprecipitation studies of skeletal-muscle lysates from WT mice treated with IP insulin (1 U/kg) for 15 min (INS 15′) and 60 min (INS 60′) in presence of β5 blocking or control antibody. Western blots are representative of three independent experiments (three mice total per condition). (*G*) Densitometric analysis of Western blots (including *F*) showing fold changes in IRβ–β5 interaction relative to no treatment (NT). (*H*) Immunostaining showing colocalization of IRβ and β5 integrin in the hind-leg skeletal muscles of mice 60 min after insulin treatment (INS 60′) in presence of β5 blocking or control antibody. For all in vivo experiments, 7 to 8 wk old WT male mice were used. Data analyzed by ANOVA followed by Bonferroni's posttest. $^{*}P < 0.05$, $^{**}P < 0.01$, and $^{***}P < 0.001$. (*I*) Proposed model showing how enhanced interaction between IRβ and β5 impedes insulin signaling.

or isotype control antibody. Insulin treatment enhanced the colocalization of IRβ and β5 (Fig. 5*H*). β5 blockade dampened the colocalization signal after insulin treatment (Fig. 5*H*), corroborating the data from coimmunoprecipitation experiments (Fig. 5 *F* and *G*). Taken together, these data indicate that insulin and MFGE8 enhance the interaction between the αvβ5 integrin and IRβ. (Fig. 5*I*).

Insulin Causes Cell-Surface Enrichment of MFGE8. We were next interested in investigating whether insulin acts as an upstream modulator of the MFGE8/β5 integrin pathway. We first examined whether insulin induces cellular secretion of MFGE8 in differentiated C2C12 myotubes. We found no differences in MFGE8 protein levels with insulin treatment with or without β5 blockade (*SI Appendix*, Fig. S8 *A* and *B*). Furthermore, we did not observe any significant fluctuations in serum or skeletal-muscle MFGE8 levels in mice during the course of an insulin tolerance test (ITT) (*SI Appendix*, Fig. S8 *C* and *D*).

We then tested whether insulin promotes MFGE8 localization at the outer cell surface, where it can bind to and activate integrin receptors. We performed cell fractionation on skeletal muscles harvested from WT mice after insulin administration. Interestingly, we observed enriched levels of MFGE8 in the plasma membrane 30, 45, and 60 min after insulin stimulation and a corresponding

decrease in the intracellular pool of MFGE8 (Fig. 6 *A* and *B*).). However, we found minimal differences in surface-membrane MFGE8 15 min after insulin treatment compared to the untreated group. Taken together, these data suggest why blocking the MFGE8/β5 pathway impacts later phases of the ITT without affecting the earlier time points. We confirmed the accuracy of our cellular fractionation technique by Western blotting individual fractions for markers of the endoplasmic reticulum (ER; BiP), Golgi (STX), cytoplasm (HSP90), and plasma membrane (CAV-1) (Fig. 6*C*).

To investigate the underlying mechanism of MFGE8 movement to the cell surface, we treated C2C12 myotubes with insulin for 30 min with or without administration of Golgicide A (GCA). GCA is a highly selective and reversible inhibitor of Cis-Golgi protein Golgi-specific brefeldin-resistance guanine nucleotide exchange factor-1 (GBF-1). GBF-1 coordinates the assembly and transport of vesicles through the ER–Golgi network (51). We then incubated cells with cell-impermeable biotin to selectively biotinylate cell-surface proteins, purified protein from lysates using a streptavidin column, and western blotted for MFGE8. Insulin increased the relative abundance of biotinylated and reduced the abundance of nonbiotinylated MFGE8 (Fig. 6 *D–F*). Moreover, pretreatment with GCA significantly reduced the cell-surface level of MFGE8 in the presence of insulin indicating that insulin stimulates MFGE8 translocation through the ER–Golgi pathway (Fig. 6 *D–F*). Successful inhibition of GBF-1 by GCA treatment was confirmed by reduced cell-surface level of ABCA1 transporter (51–53) (Fig. 6*D*).

Previous studies suggested that AMP-activated protein kinase (AMPK) regulates GBF-1 activity through phosphorylation of GBF-1 at its Thr-1333 residue (54). To understand whether insulin affects GBF-1–dependent transport of MFGE8 via regulation of AMPK, we pretreated cells with AMPK activator AICAR for 2 h and then treated cells with insulin for 30 min and performed cell-surface biotinylation assay described above. AICAR treatment dampened the insulin-mediated enrichment of cell-surface level of MFGE8 (Fig. 6 *G–I*), indicating that AMPK modulates GBF-1–dependent vesicular transport of MFGE8 from the ER–Cis-Golgi face to the cell membrane. AICAR-mediated activation of AMPK was confirmed by an AMPK activity assay (*SI Appendix*, Fig. S9). The AMPK activity assay also showed a reduction in AMPK activity in insulin-treated cells (*SI Appendix*, Fig. S9), suggesting that insulin-dependent reduction in AMPK activity activates GBF-1, which in turn, enhances the transport of MFGE8 to the cell surface. Taken together, these data indicate that insulin enriches MFGE8 at the plasma membrane of skeletal muscle cells, thus enhancing its ability to bind and activate the αvβ5 integrin (Fig. 6*J*).

Metabolic Regulation of MFGE8. We were next interested in understanding the physiological regulation of MFGE8 under different metabolic states. We therefore evaluated blood glucose, serum insulin, and serum MFGE8 levels in mice under fed, fasted (5 and 16 h), and refed states (1 h after 5 or 16 h of fasting). We found a direct correlation between serum glucose, insulin, and MFGE8

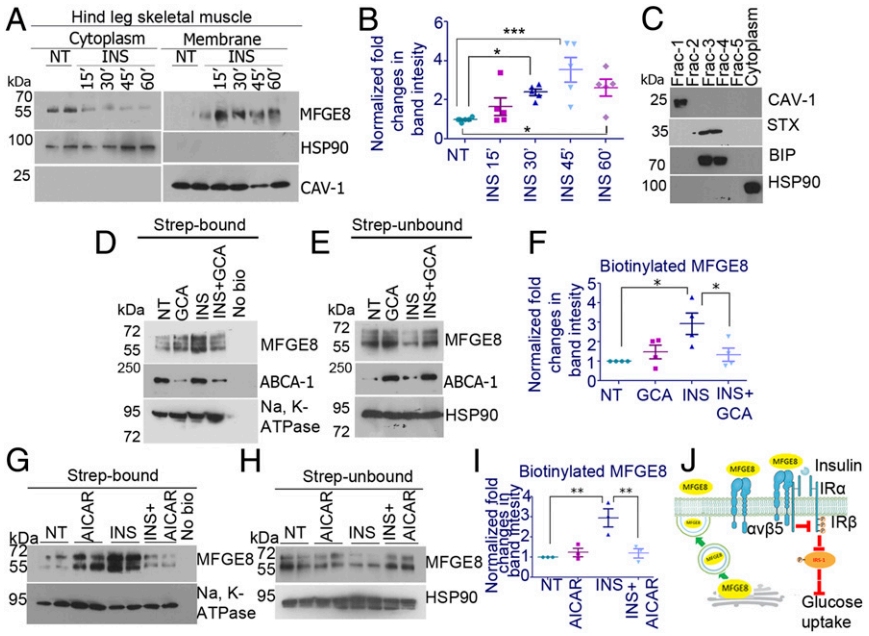

Fig. 6. Insulin induces cell-surface enrichment of MFGE8. (*A–C*) Cell fractionation of insulin-treated (1U/kg IP) skeletal-muscle tissue samples followed by Western blotting showing (*A*) MFGE8 expression in the cytoplasmic and cell-surface membrane fraction. Western blotting for HSP90 and CAVEOLIN-1 (CAV-1) confirmed cytoplasmic and membrane fractions, respectively. Western blots are representative of five independent experiments. (*B*) Densitometric analysis of Western blots (including *A*) showing relative fold changes in membrane MFGE8 in insulin-treated groups compared to NT. (*C*) Western blot showing surface membrane (CAV-1), ER (BIP), Golgi (STX) and cytoplasmic (HSP90) marker expression in different fractions from ultracentrifugation. Fraction 1 represents the cell-surface membrane used in *A*. WT male mice were used for all in vivo experiments. (*D–F*) Western blot showing cell-surface (streptavidin-bound) (*D*) and intracellular (streptavidin-unbound) (*E*) MFGE8 protein levels before and after 30 min of insulin (100 nM) treatment (INS) in C2C12 myotubes pretreated with either GCA (20 μM) or DMSO. Western blots are representative of four independent experiments. Western blotting for ABCA-1 confirmed successful inhibition of GBF-1 by GCA. (*F*) Densitometric analysis of Western blots (including *D*) showing fold changes in streptavidin-bound MFGE8 relative to NT. (*G* and *H*) Western blot showing cell-surface (streptavidin-bound, *G*) and intracellular (streptavidin-unbound, *H*) MFGE8 protein levels before and after 30 min of insulin (100 nM) treatment (INS) in C2C12 myotubes pretreated with either AICAR (10 mM) or DMSO. Data represents three independent experiments. (*I*) Densitometric analysis of Western blots (including *G*) showing fold changes in streptavidin-bound MFGE8 relative to NT. For all biotinylation experiments (*D*, *E*, *G*, and *H*), streptavidin-bound and unbound fractions were probed for HSP90 as a control for the intracellular (streptavidin-unbound) and Na,K-ATPase for the membrane-bound (streptavidin-bound) fractions. Total cell lysates not exposed to biotin reagent served a negative control (No bio). Densitometric data (*B*, *F*, and *I*) were analyzed by one-way ANOVA followed by Bonferroni's posttest. $*P < 0.05$, $**P < 0.01$, and $***P < 0.001$. (*J*) Proposed model showing how cell-surface enrichment of MFGE8 impedes insulin receptor signaling via ligation of β5 integrin.

levels (Fig. 7 *A*–*C*) with each decreasing in the fasting states and increasing in the fed states. To examine whether refeeding, which increased both serum insulin and MFGE8, impacted the interaction between β5 and IRβ in vivo, we performed coimmunoprecipitation studies of skeletal muscle tissue lysates (Fig. 7*D*). Refeeding markedly enhanced the interaction between β5 and IRβ as compared with the fasting state (Fig. 7 *D* and *E*). These data indicate that MFGE8 and the interaction between β5 and IRβ are regulated by intermediary metabolic inputs linked to fasting and refeeding.

Discussion

Insulin resistance is an underlying causative factor that predicts an individual's progression toward T2D. T2D, in turn, is a major cardiovascular disease risk factor, and cardiovascular disease is the leading cause of death among those with T2D (55). Insulin remains the only uniformly effective treatment for type I diabetes and is also a critical component of the therapeutic arsenal for T2D, especially in the face of disease progression. However, chronic insulin treatment in the context of T2D, particularly in obese individuals, can be problematic. For one, insulin-resistant individuals often require exceptionally high doses of insulin, increasing the likelihood of serious consequences when dosing errors are made. Additionally, chronic insulin treatment is associated with weight gain, which can exacerbate the obesity that fuels an individual's insulin resistance in the first place. Finally, long-term treatment with high doses of insulin could theoretically produce untoward consequences through its mitogenic effects, especially in acknowledgment that obesity is a known risk factor for a variety of cancers. For all of these reasons, it would be useful to have more effective approaches to avoid the use of insulin in patients with T2D or at least the means to improve insulin sensitivity sufficiently to allow individuals to reduce their overall daily insulin dose.

Integrins are cell-surface receptors that mediate bidirectional signaling between the cell and the extracellular environment. The main body of literature examining the effect of integrins on insulin signaling has focused on β1 integrin complexes. These data have identified important roles for these integrins in obesity-associated insulin resistance through mechanisms likely related to the physical consequences of fat expansion (26–30). By contrast, the data presented here demonstrate a direct effect of both MFGE8 and the αvβ5 integrin on insulin signaling that is independent of the effects of *Mfge8* deletion on fat mass and that is apparent even in the absence of obesity (56). This phenotype is revealed by acute antibody-dependent β5 or MFGE8 blockade in WT mice. Interestingly, the phenotype is not apparent in mice genetically lacking MFGE8 from birth (before the onset of differences in body composition at 10 wk of age), likely due to the induction of compensatory mechanisms.

Binding of insulin to the insulin receptor activates its intrinsic tyrosine kinase activity via receptor autophosphorylation and consequent phosphorylation of downstream signaling substrates. The delayed recovery of serum glucose levels we observed in the ITT after integrin blockade is strikingly similar to what is observed in ITT experiments in mice lacking the phosphatase PTP1B (10, 57). PTP1B is a well-established inhibitor of insulin receptor signaling that dephosphorylates IRβ and IRS-1. These data, coupled with the increase in the interaction between the β5 and IRβ after insulin stimulation, led us to consider whether β5 dampens and/or terminates insulin receptor signaling. Our in vitro and in vivo data in skeletal muscle and the liver demonstrating persistent phosphorylation of IRβ and IRS-1 with β5 blockade are consistent with this hypothesis. Of note, the time course of these differences is somewhat different in each organ system, which is likely the result of the more complex role the liver plays in glucose homeostasis.

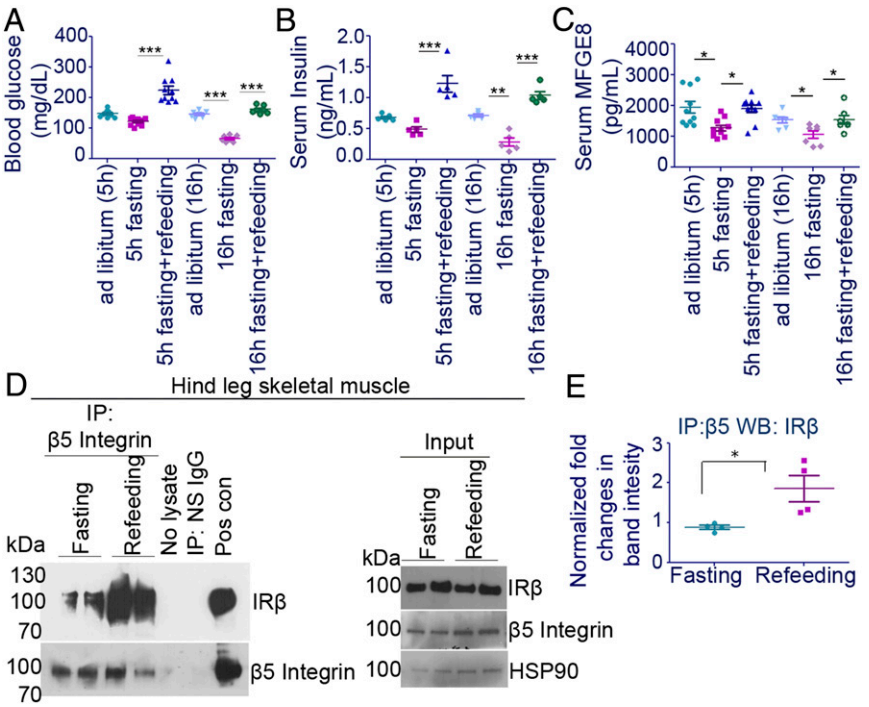

Fig. 7. Metabolic regulation of serum MFGE8 levels. (*A*–*C*) Blood glucose (*A*), serum insulin (*B*), and serum MFGE8 (*C*) levels in WT mice subjected to fasting for 5 and 16 h before a refeeding period of 1 h. $n = 7$ to 10 mice in *A* and *C*, $n = 5$ mice for *B*. Both male and female mice were used for these experiments. Data are from two to three independent experiments. (*D*) Coimmunoprecipitation experiments using hind-leg skeletal muscle lysates showing an interaction between IRβ and β5 in 16 h fasted mice and mice refed for 1 h after a 16 h fast. Data represents two independent experiments (four mice total per condition). WT male mice were used for this experiment. (*E*) Densitometric analysis of Western blots (including *D*) showing fold changes in IRβ–β5 interaction in the refed state relative to the fasted condition. Densitometry data were analyzed by Student's *t* test. Data in *A*–*C* were analyzed by one-way ANOVA followed by Bonferroni's posttest. $^*P < 0.05$, $^{**}P < 0.01$, and $^{***}P < 0.001$.

Whether these effects are through regulation of protein phosphatase or kinase activity remains to be determined. Alternatively, we can speculate the potential for a physical interaction between the integrin and the insulin receptor that, in the presence of ligand, induces structural changes in the insulin receptor that dampen its intrinsic tyrosine kinase activity.

An effect of insulin on MFGE8 protein production as a mechanism for our phenotype seems unlikely given the relatively rapid timeframe (30 min) within which we see MFGE8 impact insulin-stimulated glucose uptake. While we did not find an effect of insulin on MFGE8 secretion, insulin caused enrichment of cell membrane MFGE8 leading us to hypothesize that insulin modulates intracellular transport of MFGE8. GBF-1 coordinates the movement of proteins predominantly at the ER–cis-Golgi face (36, 37, 58, 59). Our data are consistent with work showing that GBF-1 facilitates anterograde trafficking of extracellular matrix proteins in mouse fibroblasts and human endothelial cells (60). Previous studies concerning how GBF-1 activity is regulated by AMPK have shown inconsistent results (54, 61). While AMPK-mediated phosphorylation of GBF-1 at Thr-1333 deactivates GBF-1 leading to Golgi disassembly (54, 61), AMPK activation in human endothelial cells augments GBF-1 activity (60). In our study, AICAR-mediated AMPK activation phenocopies the effect of GBF-1 inhibition in insulin-treated myotubes suggesting that AMPK activation in the presence of insulin might have an inhibitory effect on GBF-1–dependent transport of MFGE8. As reported earlier, insulin treatment causes a reduction in AMPK activity (62–64) further supporting the hypothesis that insulin via suppression of AMPK activity triggers GBF-1–dependent transport of MFGE8 to the cell surface.

Our final sets of experiments were designed to examine whether MFGE8 is physiologically regulated by varying metabolic dietary states. Interestingly, serum MFGE8 levels closely track blood glucose and serum insulin levels in the fed, fasting, and refeeding state indicating metabolic regulation of serum MFGE8 that correlates tightly with fluctuations of endogenous insulin levels. Furthermore, the marked increase in β5-insulin receptor interaction in skeletal-muscle lysates in the refeeding state suggests that metabolic regulation of MFGE8 directly impacts skeletal muscle integrin–insulin receptor interaction. One interesting question is what the cellular source of serum MFGE8 is, and to what extent the insulin-stimulated enrichment of cell membrane MFGE8 contributes to serum levels. This is a difficult question to answer experimentally since MFGE8 is produced and secreted by multiple cell types.

Normal glucose homeostasis is arguably one of the most essential vital functions of most living organisms. Decades of research have shown multiple, sometimes redundant, levels of regulation that control homeostatic glucose metabolism and provide tight regulation of this metabolism in multiple tissues under highly varying environmental and internal physiologic states. Our work adds to this understanding by demonstrating a previously unrecognized negative feedback loop of insulin signaling that is reliant on the MFGE8/β5 pathway. This negative feedback of insulin signaling might be important at an organism-wide level, preventing dangerous excursions in glucose levels by excessive or prolonged insulin signaling. Alternatively, we might speculate this self-regulation at the receptor level of insulin signaling may be analogous to autoregulation that takes place in the excitatory receptors of neuronal synapses in which case the negative feedback is also particularly important for regional tissue physiology. In insulin signaling, negative feedback in one region of muscle may prevent deprivation of glucose from other nearby regions. Addressing such issues in the future will help us work toward a more complete understanding of all levels of the regulation of glucose metabolism in health and disease.

Whether direct targeting of MFGE8 or the β5 integrin is a viable therapeutic option for patients with diabetes mellitus remains to be determined. MFGE8 impacts a heterogeneous array of biological functions some of which, from a therapeutic viewpoint, are potentially favorable and others deleterious (65). For example, MFGE8 has multiple anti-inflammatory effects (46, 66–68), which could translate into the development of unwanted inflammation with prolonged therapeutic blockade. MFGE8 promotes wound healing, epithelial-cell proliferation, and tumor-cell progression (41, 43, 69–73). These effects could, in the setting of pathway blockade, lead to delayed wound repair in diabetics or alternatively inhibit malignant transformation and growth. The antifibrotic effects of MFGE8 in the setting of blockade could exacerbate fibrotic disease though these effects that seem to be independent of the β5 integrin (74–76). The sum impact of blocking this pathway on cardiovascular health is difficult to define. MFGE8 deficiency accentuates cardiac hypertrophy and atherosclerosis in mice (39, 40), while higher coronary artery MFGE8 expression is associated with greater risk of developing coronary artery disease in humans (38). Our own work in metabolism indicates that blockade of the MFGE8/β5 pathway leads to a reduction in fat absorption and postprandial lipemia (56, 77), two effects that would be especially beneficial for the cardiovascular health of obese, diabetic patients. Alternatively, targeting β5 may be a more attractive therapeutic avenue. In fact, Cilengitide, a dual small-molecule inhibitor of αvβ3 and αvβ5, has already been used in clinical trials for glioblastoma (78). Though global $\beta5^{-/-}$ mice develop normally (79), they are prone to age-dependent blindness (80). Whether this would be a limiting factor with biological or pharmacological blockade of β5 in diabetes patients is unclear. Finally, our work provides a potential mechanism to explain the recent observations that correlate serum MFGE8 levels with multiple indices of insulin resistance (35, 36) and the increased risk of developing diabetes in a population, in which a missense variation of *Mfge8* that increases plasma levels (37).

Materials and Methods

Mice. For all studies, 6 to 8 wk old age- and sex-matched mice in C57BL/6 background were used. $Mfge8^{-/-}$ mice were purchased from RIKEN, are in the C57BL/6 background, and have been extensively characterized (66).

GTT, ITT, and PTT. The 7 to 8 wk old mice were fasted for 5 h and then injected IP with either 2 gm/kg glucose (GTT) or 1U/kg insulin (ITT). We treated mice IP with rMFGE8 or RGE protein (1 mg/kg), β5 blocking antibody (5 mg/kg) (clone ALULA, provided by A. Atakilit, University of California San Francisco [UCSF]) or mouse isotype control antibody (clone 2H6-C2, ATCC CRL-1853), MFGE8 blocking antibody (2 mg/kg) (clone 2422; MBL life sciences, D161-3) or Armenian hamster isotype control antibody (clone eBio299Arm, ThermoFisher scientific, 14-4888-81) for 1 h before glucose or insulin administration. For PTT, 6 wk old male mice were fasted for 16 h followed by IP injection of pyruvate (2 gm/kg). Mice were treated with β5 blocking or isotype control antibody 1 h before pyruvate administration. We collected blood from the tail veins immediately before glucose or insulin or pyruvate injection and then again at regular time intervals for 2 h post glucose or insulin or pyruvate administration to measure blood glucose levels.

In Vivo 18-Fluoro-Deoxy-Glucose Deposition. Mice were imaged in a dedicated small animal PET/CT scanner (Inveon, Siemens Medical Solutions) under isoflurane (2 to 2.5%) anesthesia 1 h after 18-Fluoro-Deoxy-Glucose (18FDG) and insulin injection in the presence of control or blocking antibody. All PET/CT data were normalized to an effective 18FDG dose for analysis and display within AMIDE (81, 82) (*SI Appendix, Supplementary Methods*).

In Vitro Glucose Uptake Assay. The 2NDBG uptake assay in C2C12 myotubes, HskM, and mouse primary skeletal-muscle myotubes was performed using a commercial assay kit (Cayman chemicals). Briefly, cells were preincubated with insulin (100 nM) for 10 min followed by the addition of nonhydrolyzable fluorescent glucose analog 2NBDG (10 mg/mL) for 20 min in the same media. We then measured the fluorescent intensity of cellular 2NBDG (excitation: 488 nm and emission: 535 nm) using a plate reader. Fluorescent intensities of 2NBDG were then normalized to wheat germ agglutinin (WGA 680 or WGA 594) staining intensities (*SI Appendix, Supplementary Methods*). Detailed methods of the treatment with function blocking antibodies, inhibitor, and recombinant integrin ligands are described in *SI Appendix, Supplementary Methods*.

Treatment of Cells. C2C12 myotubes after 4 to 5 d of differentiation were washed in warm phosphate-buffered saline (PBS) and then incubated in serum-free Dulbecco's modified Eagle medium (DMEM) for 4 h before treating them with insulin (100 nM) for 15 or 30 min. For studying the dose-dependent activation of the insulin receptor pathway, C2C12 myotubes were treated with different doses of insulin (25, 50, 100, and 200 nM) for 30 min. HepG2 and primary hepatocytes were treated with 100 nm insulin for 30 min. Treatment with β5 blocking (5 μg/mL) antibody or a control antibody was administered 1 h before insulin stimulation. rMFGE8 (10 μg/mL) or RGE (10 μg/mL) control construct was added to the media concurrently with insulin. GCA (20 μM) and AICAR (10 mM) were administered 2 h before insulin stimulation. An equivalent amount of dimethyl sulfoxide (DMSO) was added to control cells. Detailed methods of cell culture, protein isolation, Western blot, coimmunoprecipitation, PLA, and cell-surface biotinylation are described in *SI Appendix*, *Supplementary Methods* and Table S1.

Acute Treatment with β5 Blocking Antibody In Vivo. We fasted mice for 4 h before treating them with β5 blocking or control antibody for 1 h. Mice were then treated with IP insulin (1 U/kg) for 15 or 60 min before harvesting the hind-leg skeletal muscle and liver tissues. Tissues were then subjected to protein isolation, membrane fraction isolation, and immunostaining (*SI Appendix*, *Supplementary Methods*).

Fasting and Refeeding of Mice. Mice were fasted for 5 or 16 h and then refed with normal chow diet for 1 h prior to obtaining samples (*SI Appendix*, *Supplementary Methods*).

Statistical Analysis. One-way ANOVA was used to compare data between multiple groups. When the ANOVA comparison was significant, further pair-wise analysis was performed using Bonferroni's posttest. For analysis of blood glucose and insulin levels over time during GTTs, ITTs, and PTTs, a two-way ANOVA for repeated measures followed by Bonferroni's posttest were used. Mann–Whitney *U* or a Student's *t* test was used to compare between two groups depending on whether the data passed normality tests. All statistical analysis was performed using GraphPad Prism 6.0. Data are represented as mean ± SEM.

Study Approval. All experiments were approved by the Institutional Animal Care and Use Committee of UCSF and the UCSF Institutional Review Board.

Data Availability. All study data are included in the article and/or *SI Appendix*.

ACKNOWLEDGMENTS. This work was supported by awards from the NIH (HL136377-01 and DK110098) to K.A. R.D. was supported by the Larry L. Hillblom Foundation Fellowship Research Grant (2019-D-004-FEL). We thank Dr. Amha Atakilit and Dr. Dean Sheppard (UCSF Lung Biology Center) for providing integrin blocking antibodies and Dr. Youngho Seo (UCSF Department of Radiology and Biomedical Imaging) for helping us in setting up PET/CT experiments. We would like to thank S. Layer for ongoing inspiration.

1. J. P. Boyle, T. J. Thompson, E. W. Gregg, L. E. Barker, D. F. Williamson, Projection of the year 2050 burden of diabetes in the US adult population: Dynamic modeling of incidence, mortality, and prediabetes prevalence. *Popul. Health Metr.* **8**, 29 (2010).
2. A. Kanno *et al.*, Compensatory hyperinsulinemia in high-fat diet-induced obese mice is associated with enhanced insulin translation in islets. *Biochem. Biophys. Res. Commun.* **458**, 681–686 (2015).
3. T. Sakumoto *et al.*, Insulin resistance/hyperinsulinemia and reproductive disorders in infertile women. *Reprod. Med. Biol.* **9**, 185–190 (2010).
4. A. Tsatsoulis, The role of insulin resistance/hyperinsulinism on the rising trend of thyroid and adrenal nodular disease in the current environment. *J. Clin. Med.* **7**, 37 (2018).
5. J. Lee, T. O'Hare, P. F. Pilch, S. E. Shoelson, Insulin receptor autophosphorylation occurs asymmetrically. *J. Biol. Chem.* **268**, 4092–4098 (1993).
6. J. Lee, P. F. Pilch, The insulin receptor: Structure, function, and signaling. *Am. J. Physiol.* **266**, C319–C334 (1994).
7. L. Schäffer, A model for insulin binding to the insulin receptor. *Eur. J. Biochem.* **221**, 1127–1132 (1994).
8. G. Wilcox, Insulin and insulin resistance. *Clin. Biochem. Rev.* **26**, 19–39 (2005).
9. P. Gual, Y. Le Marchand-Brustel, J. F. Tanti, Positive and negative regulation of insulin signaling through IRS-1 phosphorylation. *Biochimie* **87**, 99–109 (2005).
10. M. Elchebly *et al.*, Increased insulin sensitivity and obesity resistance in mice lacking the protein tyrosine phosphatase-1B gene. *Science* **283**, 1544–1548 (1999).
11. B. J. Goldstein, A. Bittner-Kowalczyk, M. F. White, M. Harbeck, Tyrosine dephosphorylation and deactivation of insulin receptor substrate-1 by protein-tyrosine phosphatase 1B. Possible facilitation by the formation of a ternary complex with the Grb2 adaptor protein. *J. Biol. Chem.* **275**, 4283–4289 (2000).
12. H. Hussain *et al.*, Protein tyrosine phosphatase 1B (PTP1B) inhibitors as potential anti-diabetes agents: Patent review (2015-2018). *Expert Opin. Ther. Pat.* **29**, 689–702 (2019).
13. Y. H. Soung, J. L. Clifford, J. Chung, Crosstalk between integrin and receptor tyrosine kinase signaling in breast carcinoma progression. *BMB Rep.* **43**, 311–318 (2010).
14. D. M. Beauvais, A. C. Rapraeger, Syndecan-1 couples the insulin-like growth factor-1 receptor to inside-out integrin activation. *J. Cell Sci.* **123**, 3796–3807 (2010).
15. W. Baron, L. Decker, H. Colognato, C. ffrench-Constant, Regulation of integrin growth factor interactions in oligodendrocytes by lipid raft microdomains. *Curr. Biol.* **13**, 151–155 (2003).
16. J. Seong, M. Huang, K. M. Sim, H. Kim, Y. Wang, FRET-based visualization of PDGF receptor activation at membrane microdomains. *Sci. Rep.* **7**, 1593 (2017).
17. Y. J. Kim, K. Jung, D. S. Baek, S. S. Hong, Y. S. Kim, Co-targeting of EGF receptor and neuropilin-1 overcomes cetuximab resistance in pancreatic ductal adenocarcinoma with integrin β1-driven Src-Akt bypass signaling. *Oncogene* **36**, 2543–2552 (2017).
18. L. Seguin *et al.*, An integrin β_3-KRAS-RalB complex drives tumour stemness and resistance to EGFR inhibition. *Nat. Cell Biol.* **16**, 457–468 (2014).
19. M. Fujita, Y. K. Takada, Y. Takada, Insulin-like growth factor (IGF) signaling requires αvβ3-IGF1-IGF type 1 receptor (IGF1R) ternary complex formation in anchorage independence, and the complex formation does not require IGF1R and Src activation. *J. Biol. Chem.* **288**, 3059–3069 (2013).
20. D. M. Cedano Prieto *et al.*, Direct integrin binding to insulin-like growth factor-2 through the C-domain is required for insulin-like growth factor receptor type 1 (IGF1R) signaling. *PLoS One* **12**, e0184285 (2017).
21. J. Saegusa *et al.*, The direct binding of insulin-like growth factor-1 (IGF-1) to integrin alphavbeta3 is involved in IGF-1 signaling. *J. Biol. Chem.* **284**, 24106–24114 (2009).
22. M. Fujita *et al.*, Cross-talk between integrin α6β4 and insulin-like growth factor-1 receptor (IGF1R) through direct α6β4 binding to IGF1 and subsequent α6β4-IGF1-IGF1R ternary complex formation in anchorage-independent conditions. *J. Biol. Chem.* **287**, 12491–12500 (2012).
23. Y. Ling, L. A. Maile, D. R. Clemmons, Tyrosine phosphorylation of the beta3-subunit of the alphaVbeta3 integrin is required for embrane association of the tyrosine phosphatase SHP-2 and its further recruitment to the insulin-like growth factor I receptor. *Mol. Endocrinol.* **17**, 1824–1833 (2003).
24. K. Vuori, E. Ruoslahti, Association of insulin receptor substrate-1 with integrins. *Science* **266**, 1576–1578 (1994).
25. M. Schneller, K. Vuori, E. Ruoslahti, Alphavbeta3 integrin associates with activated insulin and PDGFbeta receptors and potentiates the biological activity of PDGF. *EMBO J.* **16**, 5600–5607 (1997).
26. L. Kang *et al.*, Diet-induced muscle insulin resistance is associated with extracellular matrix remodeling and interaction with integrin alpha2beta1 in mice. *Diabetes* **60**, 416–426 (2011).
27. L. Kang *et al.*, Integrin-linked kinase in muscle is necessary for the development of insulin resistance in diet-induced obese mice. *Diabetes* **65**, 1590–1600 (2016).
28. A. S. Williams *et al.*, Integrin α1-null mice exhibit improved fatty liver when fed a high fat diet despite severe hepatic insulin resistance. *J. Biol. Chem.* **290**, 6546–6557 (2015).
29. A. S. Williams *et al.*, Integrin-linked kinase is necessary for the development of diet-induced hepatic insulin resistance. *Diabetes* **66**, 325–334 (2017).
30. H. Zong *et al.*, Insulin resistance in striated muscle-specific integrin receptor beta1-deficient mice. *J. Biol. Chem.* **284**, 4679–4688 (2009).
31. R. Hanayama *et al.*, Identification of a factor that links apoptotic cells to phagocytes. *Nature* **417**, 182–187 (2002).
32. A. Khalifeh-Soltani *et al.*, α8β1 integrin regulates nutrient absorption through an Mfge8-PTEN dependent mechanism. *eLife* **5**, e13063 (2016).
33. M. Cheng *et al.*, Correlation between serum lactadherin and pulse wave velocity and cardiovascular risk factors in elderly patients with type 2 diabetes mellitus. *Diabetes Res. Clin. Pract.* **95**, 125–131 (2012).
34. F. Yu *et al.*, Proteomic analysis of aorta and protective effects of grape seed procyanidin B2 in db/db mice reveal a critical role of milk fat globule epidermal growth factor-8 in diabetic arterial damage. *PLoS One* **7**, e52541 (2012).
35. Y. Li *et al.*, Circulating milk fat globule-epidermal growth factor 8 levels are increased in pregnancy and gestational diabetes mellitus. *J. Diabetes Investig.* **8**, 571–581 (2017).
36. Y. Li *et al.*, Elevated serum milk fat globule-epidermal growth factor 8 levels in type 2 diabetic patients are suppressed by overweight or obese status. *IUBMB Life* **69**, 63–71 (2017).
37. B. R. Sapkota, D. K. Sanghera, A rare missense variant in the milk fat globule-EGF factor 8 (MFGE8) increases T2DM susceptibility and cardiovascular disease risk with population-specific effects. *Acta Diabetol.* **57**, 733–741 (2020).
38. S. Soubeyrand *et al.*, Regulation of MFGE8 by the intergenic coronary artery disease locus on 15q26.1. *Atherosclerosis* **284**, 11–17 (2019).
39. K. Q. Deng *et al.*, Restoration of circulating MFGE8 (milk fat globule-EGF factor 8) attenuates cardiac hypertrophy through inhibition of akt pathway. *Hypertension* **70**, 770–779 (2017).
40. H. Ait-Oufella *et al.*, Lactadherin deficiency leads to apoptotic cell accumulation and accelerated atherosclerosis in mice. *Circulation* **115**, 2168–2177 (2007).
41. A. Das *et al.*, Correction of MFG-E8 resolves inflammation and promotes cutaneous wound healing in diabetes. *J. Immunol.* **196**, 5089–5100 (2016).
42. W. Huang *et al.*, MFG-E8 accelerates wound healing in diabetes by regulating "NLRP3 inflammasome-neutrophil extracellular traps" axis. *Cell Death Discov.* **6**, 84 (2020).
43. A. Uchiyama *et al.*, Mesenchymal stem cells-derived MFG-E8 accelerates diabetic cutaneous wound healing. *J. Dermatol. Sci.* **86**, 187–197 (2017).

44. P. Laplante *et al*., MFG-E8 reprogramming of macrophages promotes wound healing by increased bFGF production and fibroblast functions. *J. Invest. Dermatol.* **137**, 2005–2013 (2017).
45. K. Lauber *et al*., Milk fat globule-EGF factor 8 mediates the enhancement of apoptotic cell clearance by glucocorticoids. *Cell Death Differ.* **20**, 1230–1240 (2013).
46. M. Kudo *et al*., Mfge8 suppresses airway hyperresponsiveness in asthma by regulating smooth muscle contraction. *Proc. Natl. Acad. Sci. U.S.A.* **110**, 660–665 (2013).
47. Y. B. Kim, S. E. Nikoulina, T. P. Ciaraldi, R. R. Henry, B. B. Kahn, Normal insulin-dependent activation of Akt/protein kinase B, with diminished activation of phosphoinositide 3-kinase, in muscle in type 2 diabetes. *J. Clin. Invest.* **104**, 733–741 (1999).
48. K. Cusi *et al*., Insulin resistance differentially affects the PI 3-kinase- and MAP kinase-mediated signaling in human muscle. *J. Clin. Invest.* **105**, 311–320 (2000).
49. F. Tremblay, C. Lavigne, H. Jacques, A. Marette, Defective insulin-induced GLUT4 translocation in skeletal muscle of high fat-fed rats is associated with alterations in both Akt/protein kinase B and atypical protein kinase C (zeta/lambda) activities. *Diabetes* **50**, 1901–1910 (2001).
50. A. Zorzano, M. Palacín, A. Gumà, Mechanisms regulating GLUT4 glucose transporter expression and glucose transport in skeletal muscle. *Acta Physiol. Scand.* **183**, 43–58 (2005).
51. J. B. Sáenz *et al*., Golgicide A reveals essential roles for GBF1 in Golgi assembly and function. *Nat. Chem. Biol.* **5**, 157–165 (2009).
52. S. Lin *et al*., BIG1, a brefeldin A-inhibited guanine nucleotide-exchange protein modulates ATP-binding cassette transporter A-1 trafficking and function. *Arterioscler. Thromb. Vasc. Biol.* **33**, e31–e38 (2013).
53. J. Lowery *et al*., The Sec7 guanine nucleotide exchange factor GBF1 regulates membrane recruitment of BIG1 and BIG2 guanine nucleotide exchange factors to the trans-Golgi network (TGN). *J. Biol. Chem.* **288**, 11532–11545 (2013).
54. T. Miyamoto *et al*., AMP-activated protein kinase phosphorylates Golgi-specific brefeldin A resistance factor 1 at Thr1337 to induce disassembly of Golgi apparatus. *J. Biol. Chem.* **283**, 4430–4438 (2008).
55. A. S. Go *et al*.; American Heart Association Statistics Committee and Stroke Statistics Subcommittee, Executive summary: Heart disease and stroke statistics–2013 update: A report from the American heart association. *Circulation* **127**, 143–152 (2013).
56. A. Khalifeh-Soltani *et al*., Mfge8 promotes obesity by mediating the uptake of dietary fats and serum fatty acids. *Nat. Med.* **20**, 175–183 (2014).
57. E. Panzhinskiy, J. Ren, S. Nair, Protein tyrosine phosphatase 1B and insulin resistance: Role of endoplasmic reticulum stress/reactive oxygen species/nuclear factor kappa B axis. *PLoS One* **8**, e77228 (2013).
58. T. Szul *et al*., Dissecting the role of the ARF guanine nucleotide exchange factor GBF1 in Golgi biogenesis and protein trafficking. *J. Cell Sci.* **120**, 3929–3940 (2007).
59. X. Zhao *et al*., GBF1, a cis-Golgi and VTCs-localized ARF-GEF, is implicated in ER-to-Golgi protein traffic. *J. Cell Sci.* **119**, 3743–3753 (2006).
60. M. Lopes-da-Silva *et al*., A GBF1-dependent mechanism for environmentally responsive regulation of ER-golgi transport. *Dev. Cell* **49**, 786–801.e6 (2019).
61. L. Mao *et al*., AMPK phosphorylates GBF1 for mitotic Golgi disassembly. *J. Cell Sci.* **126**, 1498–1505 (2013).
62. S. A. Hawley *et al*., Phosphorylation by Akt within the ST loop of AMPK-α1 down-regulates its activation in tumour cells. *Biochem. J.* **459**, 275–287 (2014).
63. S. M. Jeon, Regulation and function of AMPK in physiology and diseases. *Exp. Mol. Med.* **48**, e245 (2016).
64. R. J. Valentine, K. A. Coughlan, N. B. Ruderman, A. K. Saha, Insulin inhibits AMPK activity and phosphorylates AMPK Ser(4)(8)(5)/(4)(9)(1) through Akt in hepatocytes, myotubes and incubated rat skeletal muscle. *Arch. Biochem. Biophys.* **562**, 62–69 (2014).
65. B. Z. Li, H. Y. Zhang, H. F. Pan, D. Q. Ye, Identification of MFG-E8 as a novel therapeutic target for diseases. *Expert Opin. Ther. Targets* **17**, 1275–1285 (2013).
66. R. Hanayama *et al*., Autoimmune disease and impaired uptake of apoptotic cells in MFG-E8-deficient mice. *Science* **304**, 1147–1150 (2004).
67. K. Atabai *et al*., Mfge8 is critical for mammary gland remodeling during involution. *Mol. Biol. Cell* **16**, 5528–5537 (2005).
68. N. Deroide *et al*., MFGE8 inhibits inflammasome-induced IL-1β production and limits postischemic cerebral injury. *J. Clin. Invest.* **123**, 1176–1181 (2013).
69. H. F. Bu *et al*., Milk fat globule-EGF factor 8/lactadherin plays a crucial role in maintenance and repair of murine intestinal epithelium. *J. Clin. Invest.* **117**, 3673–3683 (2007).
70. L. Tibaldi *et al*., New blocking antibodies impede adhesion, migration and survival of ovarian cancer cells, highlighting MFGE8 as a potential therapeutic target of human ovarian carcinoma. *PLoS One* **8**, e72708 (2013).
71. M. Neutzner *et al*., MFG-E8/lactadherin promotes tumor growth in an angiogenesis-dependent transgenic mouse model of multistage carcinogenesis. *Cancer Res.* **67**, 6777–6785 (2007).
72. D. S. Ko *et al*., Milk fat globule-EGF factor 8 contributes to progression of hepatocellular carcinoma. *Cancers (Basel)* **12**, 403 (2020).
73. M. Jinushi *et al*., Milk fat globule EGF-8 promotes melanoma progression through coordinated Akt and twist signaling in the tumor microenvironment. *Cancer Res.* **68**, 8889–8898 (2008).
74. S. Y. An *et al*., Milk fat globule-EGF factor 8, secreted by mesenchymal stem cells, protects against liver fibrosis in mice. *Gastroenterology* **152**, 1174–1186 (2017).
75. Y. J. Jang, S. Y. An, J. H. Kim, Identification of MFGE8 in mesenchymal stem cell secretome as an anti-fibrotic factor in liver fibrosis. *BMB Rep.* **50**, 58–59 (2017).
76. K. Atabai *et al*., Mfge8 diminishes the severity of tissue fibrosis in mice by binding and targeting collagen for uptake by macrophages. *J. Clin. Invest.* **119**, 3713–3722 (2009).
77. A. Khalifeh-Soltani *et al*., Mfge8 regulates enterocyte lipid storage by promoting enterocyte triglyceride hydrolase activity. *JCI Insight* **1**, e87418 (2016).
78. R. Stupp *et al*.; European Organisation for Research and Treatment of Cancer (EORTC); Canadian Brain Tumor Consortium; CENTRIC study team, Cilengitide combined with standard treatment for patients with newly diagnosed glioblastoma with methylated MGMT promoter (CENTRIC EORTC 26071-22072 study): A multicentre, randomised, open-label, phase 3 trial. *Lancet Oncol.* **15**, 1100–1108 (2014).
79. X. Huang, M. Griffiths, J. Wu, R. V. Farese Jr, D. Sheppard, Normal development, wound healing, and adenovirus susceptibility in beta5-deficient mice. *Mol. Cell. Biol.* **20**, 755–759 (2000).
80. E. F. Nandrot *et al*., Loss of synchronized retinal phagocytosis and age-related blindness in mice lacking alphavbeta5 integrin. *J. Exp. Med.* **200**, 1539–1545 (2004).
81. M. C. Kreissl *et al*., Influence of dietary state and insulin on myocardial, skeletal muscle and brain [F]-fluorodeoxyglucose kinetics in mice. *EJNMMI Res.* **1**, 8 (2011).
82. A. M. Loening, S. S. Gambhir, AMIDE: A free software tool for multimodality medical image analysis. *Mol. Imaging* **2**, 131–137 (2003).